

# RSC Advances



This is an *Accepted Manuscript*, which has been through the Royal Society of Chemistry peer review process and has been accepted for publication.

*Accepted Manuscripts* are published online shortly after acceptance, before technical editing, formatting and proof reading. Using this free service, authors can make their results available to the community, in citable form, before we publish the edited article. This *Accepted Manuscript* will be replaced by the edited, formatted and paginated article as soon as this is available.

You can find more information about *Accepted Manuscripts* in the [Information for Authors](#).

Please note that technical editing may introduce minor changes to the text and/or graphics, which may alter content. The journal's standard [Terms & Conditions](#) and the [Ethical guidelines](#) still apply. In no event shall the Royal Society of Chemistry be held responsible for any errors or omissions in this *Accepted Manuscript* or any consequences arising from the use of any information it contains.

## Calcite Precipitation from By-Product Red Gypsum in Aqueous Carbonation Process

Cite this: DOI: 10.1039/x0xx00000x

Omeid Rahmani <sup>\* a,b</sup>, Mark Tyrer <sup>c</sup> and Radzuan Junin <sup>a</sup>

Received 18th June 2014  
Accepted 00th September 2014

DOI: 10.1039/x0xx00000x

[www.rsc.org/](http://www.rsc.org/)

The carbon dioxide (CO<sub>2</sub>) concentration of the atmosphere has been increasing rapidly, and this rapid change has led to promotion of CO<sub>2</sub> reduction methods. Of all the available methods, CO<sub>2</sub> mineral carbonation provides a leakage-free option to produce environmentally benign and stable solid carbonates via a chemical conversion to a more thermodynamically stable state. In this research, the precipitation of calcite from by-product red gypsum was evaluated for mineral CO<sub>2</sub> sequestration. For this purpose, the impact of changing variables such as reaction temperature, particle size, stirring rate, and liquid to solid ratio were studied. The results showed that optimization of these variables converts the maximum Ca (98.8%) during the carbonation process. Moreover, the results confirmed that red gypsum has a considerable potential to form calcium carbonate (CaCO<sub>3</sub>) during CO<sub>2</sub> mineral carbonation process. Furthermore, the low cost and small amount of energy required in the use of by-product red gypsum were considered to be important advantages of the CO<sub>2</sub> sequestration process. Therefore, the acceptable cost and energy required in mineral carbonation processing of red gypsum confirms that using this raw material represents a method for mineral carbonation with minimal environmental impact.

## Introduction

Increasing greenhouse gases concentration, especially CO<sub>2</sub>, is the most significant factor influencing global temperature increases. To minimize the impact of CO<sub>2</sub> emissions, concentrations of CO<sub>2</sub> should be stabilized by reducing its release into the atmosphere [1]. There are several methods established for CO<sub>2</sub> sequestration such as geologic storage and ocean storage [2,3], and mineral carbonation. Among these various approaches, mineral carbonation is considered to be an interesting method that involves the process by which CO<sub>2</sub> is removed from the atmosphere and is sequestered in stable minerals that are formed through its reaction [4-6]. Common elements which can be used for mineral carbonation are calcium (Ca) and magnesium (Mg), where atmospheric CO<sub>2</sub> reacts with Ca<sup>2+</sup> or Mg<sup>2+</sup> to form solid carbonates [7-14]. Many industrial wastes such as lignite fly ash, mining waste, and steel slag containing large amounts of Ca<sup>2+</sup>/Mg<sup>2+</sup> have been evaluated as potential raw materials for CO<sub>2</sub> sequestration processing [10-11]. However, red gypsum is a new Ca-rich feedstock that has not yet been addressed for mineral carbonation processing. This study focused on the reaction of by-product red gypsum because it is readily available in Malaysia and is mostly deposited into landfills (e.g., landfill of Huntsman Tiioxide, Terengganu). Huntsman Tiioxide is one of the world's largest producers of TiO<sub>2</sub> pigments. The capacity of its plant in Malaysia is about 56,000 metric tonne per year [10]. The titanium dioxide industry in Malaysia produces 1 million t of red gypsum annually that could be utilized for CO<sub>2</sub> sequestration [10]. This industrial by-product contains approximately 32.2% CaO [10,11], which makes it a potential feedstock for mineral carbonation purposes. According to Claisse et al. [15], red gypsum, which contains approximately 75% gypsum and 25% iron, is an omnipresent feedstock in industrialized societies. Red gypsum is a by-product of titanium dioxide (TiO<sub>2</sub>) production using sulfate processing [15]. The addition of limestone during flue gas desulfurization produces gypsum, which along with that precipitated during acid neutralization are the main sources for by-product red gypsum production.

The main objectives of the current study are:

- (1) To determine the rate of dissolution and carbonation of red gypsum in order to optimize the process of mineral CO<sub>2</sub> sequestration and to test the effect of variables such as reaction temperature, stirring rate, liquid to solid ratio, and particle size.
- (2) To determine the cost and energy required in dissolution and in the carbonation of red gypsum and to assess the environmental issues associated with mineral CO<sub>2</sub> sequestration.

## Experimental Section

### Materials

More than five kilograms of red gypsum, as a main raw material, were obtained from the local landfill of Huntsman Tiioxide, Terengganu, Malaysia. Characterization of fresh red gypsum samples and the resulting products was performed using X-ray fluorescence (XRF, PW-1410 Philips), X-ray diffraction (XRD, X'Pert-MPD Philips), field emission scanning electron microscopy (FESEM, SU8200 Hitachi), energy dispersive X-ray spectrometer (EDX), and inductively coupled plasma mass spectrometry (ICP-MS, 4500 HP) analyses. Furthermore, the particle size of the by-product red gypsum samples was measured with a particle size analyzer (Micrometrics

ASAP-2020). The final product phases were also determined using XRD and thermogravimetric (TGA, Q500) analyses.

The collected samples were dried in an oven at 45 °C for 24 h to remove surface water but prevent dehydration. To dissolve the Ca and Fe components in red gypsum sample, different amounts of sulfuric acid (H<sub>2</sub>SO<sub>4</sub>) at different concentrations were used. Numerous tests were conducted in this study to establish the optimum amount and concentration of H<sub>2</sub>SO<sub>4</sub>, which are 1.5 M and 35%, respectively. Subsequently, different amount of ammonium hydroxide (NH<sub>4</sub>OH) were tested to extract the Fe and then the Ca components from solution. In this study, the optimum amount of NH<sub>4</sub>OH is 2.1 M.

### Experimental apparatus

The carbonation of red gypsum samples was carried out in a 150 ml reactor. To set up the instrument for mineral carbonation processing, a gas cylinder of CO<sub>2</sub> with a purity of 99.99% was attached to the reactor (Fig. 1). In addition, a CO<sub>2</sub> flow-meter regulator (HPT-GAR-398CR Hero) was installed to the cylinder to control the flow rate of injected CO<sub>2</sub> and calculate the net volume (%) of inlet gas. Moreover, a hose that was 2 m in length and 6.4 mm in diameter was connected to both the flow-meter regulator and the reactor. A digital set reactor controller with a hall sensor feedback (input power supply: 220 V; 50Hz) was embedded in the reactor to control stirring speed and temperature. CO<sub>2</sub> was introduced into the reactor at different partial pressures (up to 30%) and combined with solution rich in Ca and NH<sub>4</sub>OH.

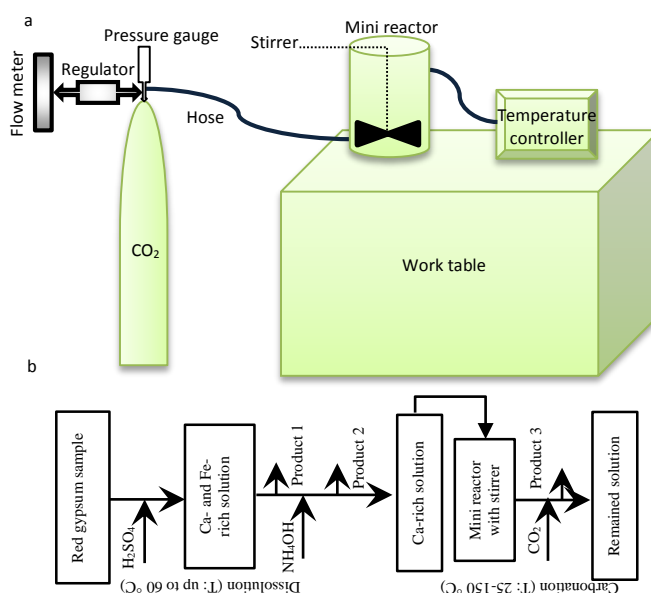


**Fig. 1** (A) A schematic diagram of experimental set-up and (b) its procedure.

### Experimental procedure

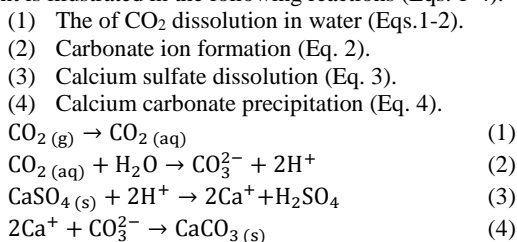
The dissolution process includes two stages: impurity removal and metal extraction. At the beginning of the dissolution experiment, 10 grams of dried red gypsum sample with a defined particle size of <75 µm was poured into a beaker and dissolved in 1.5 M H<sub>2</sub>SO<sub>4</sub> (equal to ~143 ml in concentration of 35%). The dissolution experiment was performed using a magnetic stir bar at a temperature of 60 °C and a pressure of 1 atm in a batch water heater. Two hours after the H<sub>2</sub>SO<sub>4</sub> was added to the fresh red gypsum sample, the first residual product

was removed from the solution after sedimentation and then filtration. The Ca- and Fe-rich solution was filtered to separate undissolved and impure particles. Therefore, the main aim of using H<sub>2</sub>SO<sub>4</sub> was to remove impurities and extract Fe as the main metal from red gypsum samples.

Because a surplus of H<sub>2</sub>SO<sub>4</sub> was used for dissolving by-product red gypsum samples, the solution that was formed was acidic (pH ~2.5). Therefore, in the second stage, an amount (100 ml of 2.1 M NH<sub>4</sub>OH) of ammonia was added to the Ca- and Fe-rich solution to increase the pH value to 8.6 and create the second product. The dissolution experiment was also performed using a magnetic stirrer bar at ambient conditions in a beaker. At the end of this stage, Fe was extracted from the Ca- and Fe-rich solution. Because the indirect aqueous mineral carbonation of red gypsum samples are selected as the main route of carbonation process in this study, it was necessary to extract the Fe prior to CaCO<sub>3</sub> precipitation. The remaining solution is rich in Ca. Subsequently, the pH value of solid solution was increased by adding ~3 ml 2.1 M NH<sub>4</sub>OH to a pH of 9.5.

The carbonation experiment was carried out in a 150 ml autoclave mini reactor (500 mm in height and 10 mm in diameter). The reactor was overloaded with the solution before being heated. After overloading, CO<sub>2</sub> was introduced to the reactor with partial pressures ranging from 1 to 30% in the basis of increasing reaction temperature and time. A mass flow controller was used to regulate the flow of CO<sub>2</sub> gas. At the same time, the reactor was heated electrically and its temperature monitored by a thermocouple connected to the digital set reactor controller, maintaining a fixed temperature between 25 and 150 °C. Various stirring rates up to 600 rpm were applied. However, the stirring rate of 400 rpm proved to be the optimum rate to improve the dissolution of CO<sub>2</sub> in the Ca-rich solution. This was because CO<sub>2</sub> and Ca-rich solution had different densities, and thus, they formed distinct lines at higher stirring rates. At rates lower than the optimum rate, the reaction between the Ca-rich solution and the injected CO<sub>2</sub> was not significant. The carbonation experiments were performed over the course of 3 h, after which the precipitated CaCO<sub>3</sub> was separated from the solution and collected as the final product.

In the carbonation step, Ca in the solution reacted with CO<sub>2</sub> to form the third product, CaCO<sub>3</sub>. The dissolution of the Ca<sup>2+</sup> cation and then its reaction with CO<sub>2</sub> to precipitate CaCO<sub>3</sub> was considered to be an essential factor in the mineral carbonation process of red gypsum. Because the Ca<sup>2+</sup> cation is present in both the dissolution and carbonation steps, it was expected to form the stable carbonated mineral. The mechanism of CO<sub>2</sub> sequestration during the carbonation experiment is illustrated in the following reactions (Eqs. 1-4).



### Determination of Ca conversion and CO<sub>2</sub> uptake

The amount of Ca conversion (Eq. 5) was calculated from the amount of precipitated CaCO<sub>3</sub> and the amount of Ca in solution normalized to the Ca content of initial red gypsum samples. It was assumed that only Ca is carbonated during the mineral carbonation process. Moreover, the reactor was designed on the basis of no substantial material loss due to leakage.

$$\text{Ca conversion (\%)} = \frac{\text{Ca}^{2+}[(\text{precipitated as CaCO}_3) \times \text{achieved product}]}{\text{Ca}^{2+}(\text{as CaO in by-product red gypsum}) \times \text{sample used}} \times 100 \quad (5)$$

The rate of CO<sub>2</sub> uptake (mmol/g) in the system was determined by measurement of the CO<sub>2</sub> concentration of the exhaust gas using an optical IR-sensor (Vaisala, GMP221) and from known gas flue. The partial pressure of CO<sub>2</sub> was calculated from the CO<sub>2</sub> concentration measured at atmospheric gas pressures (Eq. 6).

$$\text{CO}_2 \text{ uptake (mmol/g)} = \sum_i^n \frac{(p\text{CO}_{2 \text{ in}} - p\text{CO}_{2 \text{ out}})_i * \Delta t * Q}{R * T * M} \quad (6)$$

In Equation 6,  $p\text{CO}_{2 \text{ out}}$  and  $p\text{CO}_{2 \text{ in}}$  are mean value of  $p\text{CO}_2$  in the outflow and partial pressure of CO<sub>2</sub> ranged between 10 and 30%,  $\Delta t$  and  $Q$  are time interval (min) and flow rate (L/min),  $R$  and  $T$  are gas constant (8.32J/mol\*K) and temperature (K), and  $M$  is mass of by-product red gypsum (g). Additionally, based on the amount of procedure variables such as reaction temperature, stirring rate, liquid to solid ratio, and particle size; CO<sub>2</sub> uptake in red gypsum suspension were experimentally determined.

### Energy consumption and cost analysis

The red gypsum sample was crushed to maximize the surface area of mineral available for reaction. Apart from grinding, the samples needed a temperature of up to 150 °C in order to achieve optimum results. This process consumes energy and is considered to be costly. Therefore, Bond's equation was employed for calculating the energy consumption  $W$ :

$$W = 0.01W_i \left( \frac{1}{\sqrt{d_1}} - \frac{1}{\sqrt{d_0}} \right) \quad (7)$$

In the Equation 7,  $W$  and  $W_i$  are the required energy to reduce the particle size and the experimental work index of the red gypsum in kWh/t, respectively. In addition,  $d_0$  is the original particle size while  $d_1$  accounts for the final crushed size. According to Hangx and Spiers [16], the value of work index can be determined from the hardness of raw materials. In this way, the work index for red gypsum was calculated as 10.77 kWh/t (see Supported Information A). On the other hand, to reach the final size of particle, ultra-fine grinding was done to the particles less than 38 μm and an extra multiplier (Eq. 8) was applied to Equation 7. The amount of energy consumption during grinding to 38 μm and ultra-fine grinding to 10 μm of samples was 0.185 and 0.643 kWh/t, respectively.

$$W = 0.01W_i \left( \frac{1}{\sqrt{d_1}} - \frac{1}{\sqrt{d_0}} \right) \times \frac{(10.6 \times 10^{-6} + d_1)}{1.145 d_1} \quad (8)$$

Furthermore, a preliminary cost analysis; including feedstock cost, chemical consumption, and energy consumption was developed based on the conducted experiments. It was assumed that red gypsum samples are transported approximately 100 km from the factory to storage place. According to Hangx and Spiers [16], this represents approximately 10.3 kg/tCO<sub>2</sub> embedded CO<sub>2</sub> and a cost of approximately \$7–\$15 (average \$11) per tonne of by-products.

## Results and Discussion

### Red gypsum characterization

As shown in Figure 2, XRD results showed that calcium sulfate or gypsum mineral (CaSO<sub>4</sub>·2H<sub>2</sub>O) is the dominant component in the sample (see Supported Information B). The fresh samples consists of three major components: CaO (32.20 wt.%), SO<sub>3</sub> (31.60 wt.%), and Fe<sub>2</sub>O<sub>3</sub> (28.99 wt.%), in addition to a high portion of TiO<sub>2</sub> (5.64 wt.%), which was determined by XRF analysis (Table 1). Unsurprisingly, the

main constituents of the samples were comparable to those detected in Fauziah *et al.* [17]. The high portions of CaO and SO<sub>3</sub> in the mineral composition of red gypsum samples confirmed that they could be considered as a potential feedstock for the mineral carbonation process. Therefore, it is important to focus on these two main components. It is also significant to note the high content of TiO<sub>2</sub> in the mineral composition of red gypsum samples. According to Gazquez *et al.* [18], it is not surprising to detect a high amount of TiO<sub>2</sub> in by-product red gypsum (i.e., ~5%), the recovery of which could lead to a substantial improvement in the industrial process efficiency. Furthermore, this by-product contains a large amount of hydrated Fe<sub>2</sub>O<sub>3</sub> which accounts for its distinct red color. In addition, the fresh sample includes very low amounts of impurities such as Hg, Zn, Cu, and Cr (conducted by ICP-MS) representing substantially less than 1 wt. % of the total and these were not considered to be significant. Moreover, the red gypsum sample was analyzed for trace element concentrations using ICP-MS. The evaluation of the major components confirmed that there was uniformity in the composition of the red gypsum. In addition, the composition uniformity of the samples was replicated in the trace elements study.

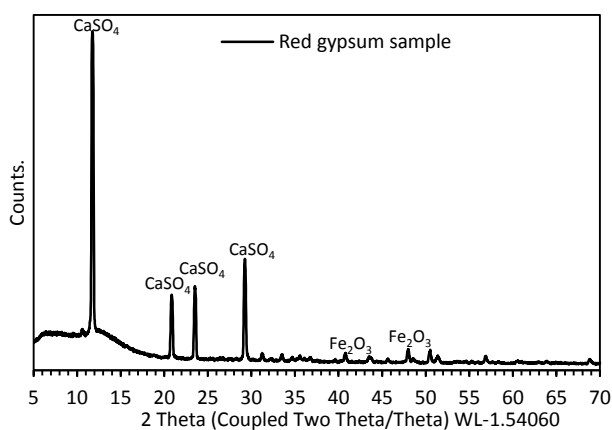


**Fig. 2** X-ray diffraction of bulk red gypsum sample.

**Table 1** Chemical composition of fresh red gypsum sample, conducted by XRF in major components and by ICP-MS in minor components and trace elements

Major component (wt.%)		Trace elements (ppm)	
CaO	32.20	V	443.5
SO <sub>3</sub>	31.60	Cr	117.5
Fe <sub>2</sub> O <sub>3</sub>	28.99	Co	11.5
TiO <sub>2</sub>	5.640	Ni	35.0
		Cu	256.0
		Zn	239.0
Minor component (wt.%)		As	11.5
MnO	0.410	Zr	267.0
Al <sub>2</sub> O <sub>3</sub>	0.390	Nb	116.0
Eu <sub>2</sub> O <sub>3</sub>	0.260	Cd	1.4
V <sub>2</sub> O <sub>5</sub>	0.220	Sc	11.5
CuO	0.063	Pt	109.0
ZnO	0.040	Ce	113.0
SrO	0.032	Pb	36.0
Cr <sub>2</sub> O <sub>3</sub>	0.032	Th	32.5
HgO	0.030	Ir	1.6

In addition, the particle size distribution of the red gypsum sample

was measured by particle size analysis (Fig. 3). This method uses light dispersion of particles that are suspended in water and to obtain a high-level of dispersion, these samples were stored for 24 hours prior to measurement. Subsequently, each prepared sample was introduced to a magnetic separator and was then stirred at up to 600 revolution per minute (rpm). Finally, the sample was collected and particles size distribution was measured by a laser diffraction using a MASTERSIZE 2000 system. The particle size analyzer results indicated that the particle size of samples is dominantly in the range of less than 10 to more than 100 μm. As shown in Figure 3, most particles (over 70%) are smaller than 75 μm in the samples that were analyzed. Overall, no noticeable changes were observed in the particle size distribution between the two samples.

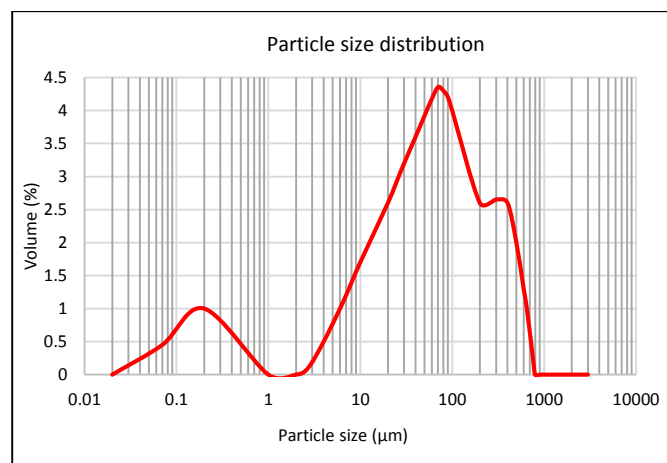


**Fig. 3** Particle size distribution of red gypsum.

### Reaction mechanisms

Figures 4-6 are FESEM photomicrographs of by-product red gypsum samples at different stages of processing. In both the dissolution and carbonation experiments, the change in the morphology of the particle surface was pronounced, as the solids converted from gypsum to calcite. We note however, that some unreacted components persist during the transformation of the bulk mineralogy, such as that shown in Figure 4a. EDX analysis showed that the unreacted particles are mainly composed of TiO<sub>2</sub>. At the end of dissolution experiment, the Ca- and Fe-rich solution was filtered via a Whatman paper for extracting the second product. EDX analysis confirmed that this waste product is rich in Fe (Fig. 4b).

After the dissolution experiment, there was a porous coating in carbonated particles that was not present on uncarbonated ones (Fig. 5a). Some unreacted particles are observed on the surface of carbonated ones. This suggests that the presence of Fe in the Ca-Fe-O phase may restricts the rate of red gypsum dissolution. Subsequently, by removing the Fe content from the solid solution as the second product, the unstable CaCO<sub>3</sub> crystals appeared. In the upper level of mineral carbonation, unstable crystals of CaCO<sub>3</sub> tended to form stable ones. Figure 5b shows the intermediate level of converted crystal symmetry from the unstable stage to the stable stage of the third product. In Figure 5c, the crystal symmetry of the third product is shown as a trigonal-rhombohedral. The chemical composition of the third product (i.e., CaCO<sub>3</sub>) was determined using X-ray diffraction (Fig. 5d). To achieve this CaCO<sub>3</sub> symmetry (i.e., stable form), the process variables were optimized as follows:

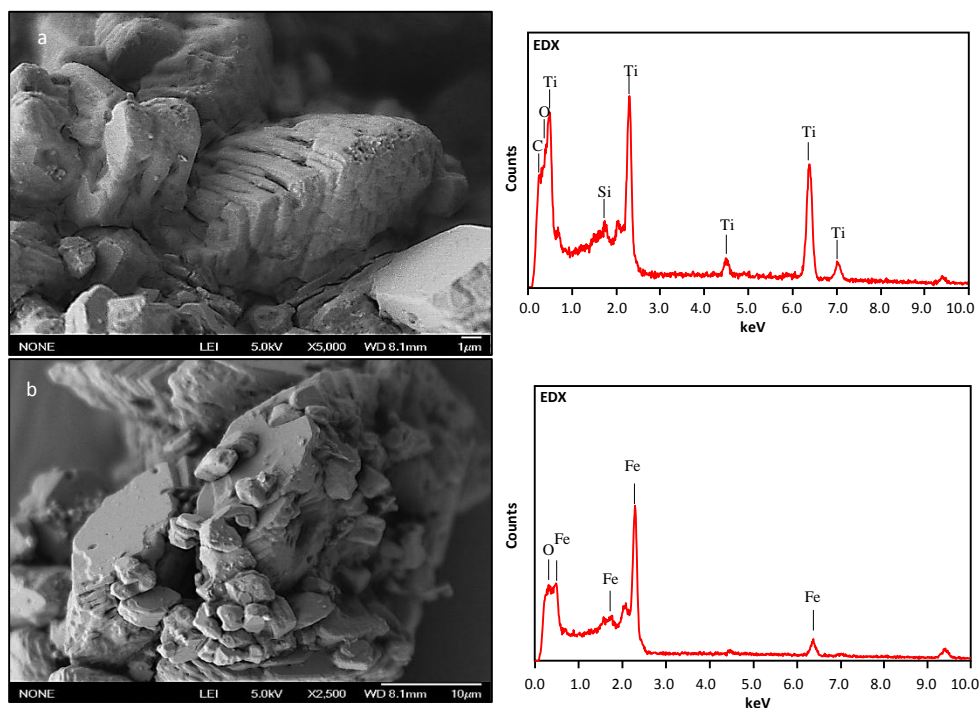


**Fig.4** FESEM photomicrographs with EDX analysis of the first (a) and second (b) products in mineral carbonation of red gypsum samples.

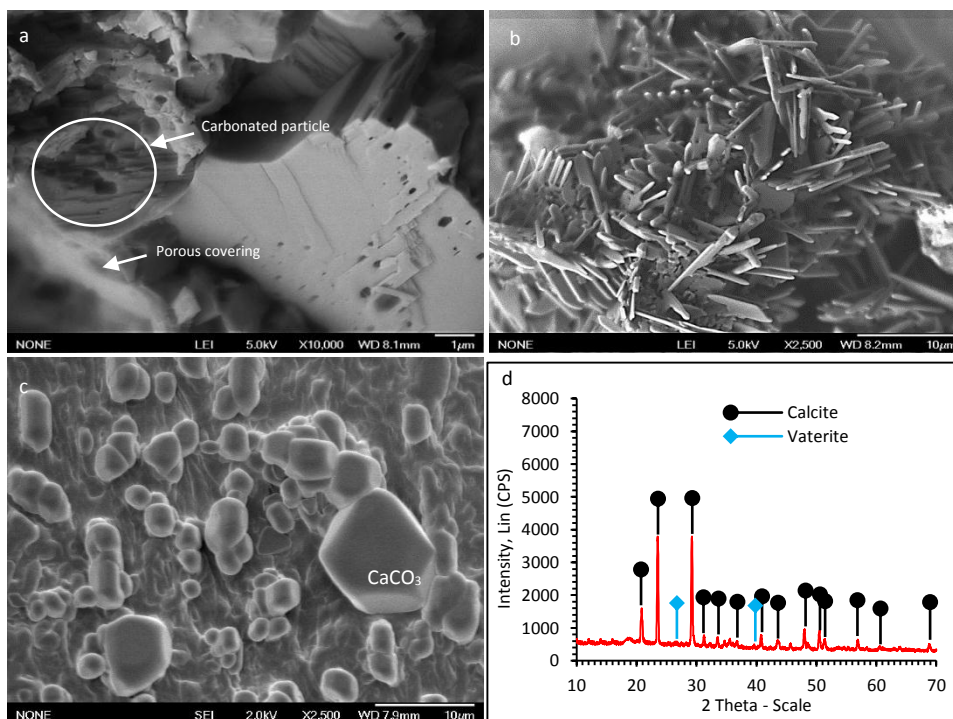


**Fig. 5** FESEM photomicrographs of (a) carbonated particle surrounded by porous coating and (b) metastable stage of the third product. The photomicrograph (c) shows the crystal symmetry of  $\text{CaCO}_3$  that is trigonal-rhombohedral. (d) X-ray diffraction analysis upon a final product sample confirmed that the chemical composition of the third product consists of  $\text{CaCO}_3$ .

**Temperature:** The dissolution rate of the samples with a mean particle size fraction of 38  $\mu\text{m}$  was verified at temperatures from 25  $^{\circ}\text{C}$  to 150  $^{\circ}\text{C}$  (Fig. 6a). As anticipated, the temperature had an important effect on the mineral carbonation process of extracting Fe and Ca and precipitation of  $\text{CaCO}_3$ . As shown in Figure 6a, the maximum amount of Ca converted to  $\text{CaCO}_3$  is 98.8%, which occurred at 60  $^{\circ}\text{C}$ . The temperatures above 60  $^{\circ}\text{C}$  had an opposite effect on the dissolution capabilities for each element that was verified. It could be concluded that the structure of gypsum is unstable at temperature above 60  $^{\circ}\text{C}$  and the decomposition of the chemical begins and the dissolution of  $\text{CO}_2$  in Ca-rich solution decreases. On the other hand, the maximum amount of Ca conversion was 75% at higher temperatures, i.e., more than 60  $^{\circ}\text{C}$ , which was considered to be an opposite effect. Therefore, when the temperature was higher than 60  $^{\circ}\text{C}$ , the amount of Ca conversion was significantly decreased.

The temperature effect indicated that three factors influence the reaction rate of  $\text{CaCO}_3$ : Ca leaching at temperature from 25  $^{\circ}\text{C}$  to 60  $^{\circ}\text{C}$ ,  $\text{CaSO}_4$  stability at temperature above 60  $^{\circ}\text{C}$ , and  $\text{CO}_2$  dissolution temperatures above 150  $^{\circ}\text{C}$ . As expected, the rate and extent of the reaction increase with increasing temperature to 60  $^{\circ}\text{C}$  because the efficiency of the reaction improved with increasing temperature to 60  $^{\circ}\text{C}$ . To translate these findings into a commercially viable process, recovery of the reaction heat from the initial stages would significantly decrease  $\text{CO}_2$  dissolution at higher temperatures.

**Stirring Rate:** Based on results of the initial tests, the maximum conversion of Ca occurs at a stirring rate of 400 rpm by considering the optimum reaction temperature (60  $^{\circ}\text{C}$ ). Increasing the stirring rate more than 400 rpm had a reverse effect on the conversion of Ca. We suggest that this is due to exsolution of gaseous  $\text{CO}_2$  (out-gassing) through mechanical agitation. Furthermore, the fast transformation of  $\text{Ca}^{2+}$  from the surface of particles into Ca-rich solution could be considered as another possible effect of stirring rate upon the conversion of Ca. It can be concluded that the particles in Ca-rich solutions tend to diffuse Ca from their inner parts to the surface, and consequently, this process controls the carbonation rate. As stirring rate increased to 400 rpm, the  $\text{CO}_2$  transfer enhanced in the Ca-rich solution to ~15.80 wt.% (Fig. 6b). This enhancement in  $\text{CO}_2$  transfer is due to rising disorder between the liquid-gas borderline.

**Liquid to Solid Ratio (L/S):** As shown in Figure 6c, the highest efficiency of Ca conversion (~98.8%) was reached with the lowest L/S ratio (10 ml/g). When the L/S ratio increased to 30 ml/g, the conversion of Ca slightly decreased to ~91%. Moreover, increasing the L/S ratio to 100 ml/g caused to a decrease in Ca conversion to 75%. Nevertheless, the L/S ratio constantly increased to 200 ml/g, and the conversion efficiency of Ca increased to 82%. Increasing the high L/S ratio increased the possibility of interactions between particles. When the product layer was developed by collision of particles, the  $\text{CaSO}_4$  particles located below the product layer could react with the reactive component (e.g.,  $\text{NH}_4\text{OH}$ ). It is suggested that increased conversion efficiency increases the diffusion of reactive components in the pore spaces of particles [19,20].

**Particle Size:** The effect of particle size was tested by applying 4 different ranges of samples in the metal extraction (dissolution) and carbonation experiments: <75, 75-125, 125-200, and >200  $\mu\text{m}$ . Figure 6d shows that decreasing the grain size from >200  $\mu\text{m}$  to <75  $\mu\text{m}$  caused the conversion rate of Ca to increase from 37% to 98.8%, respectively. Reducing particle size caused an increase in particle surface area, which resulted in enhanced reaction rates. Therefore, decreasing the average grain size by ~3 times led to a 2-fold increase in the rate of Ca conversion.

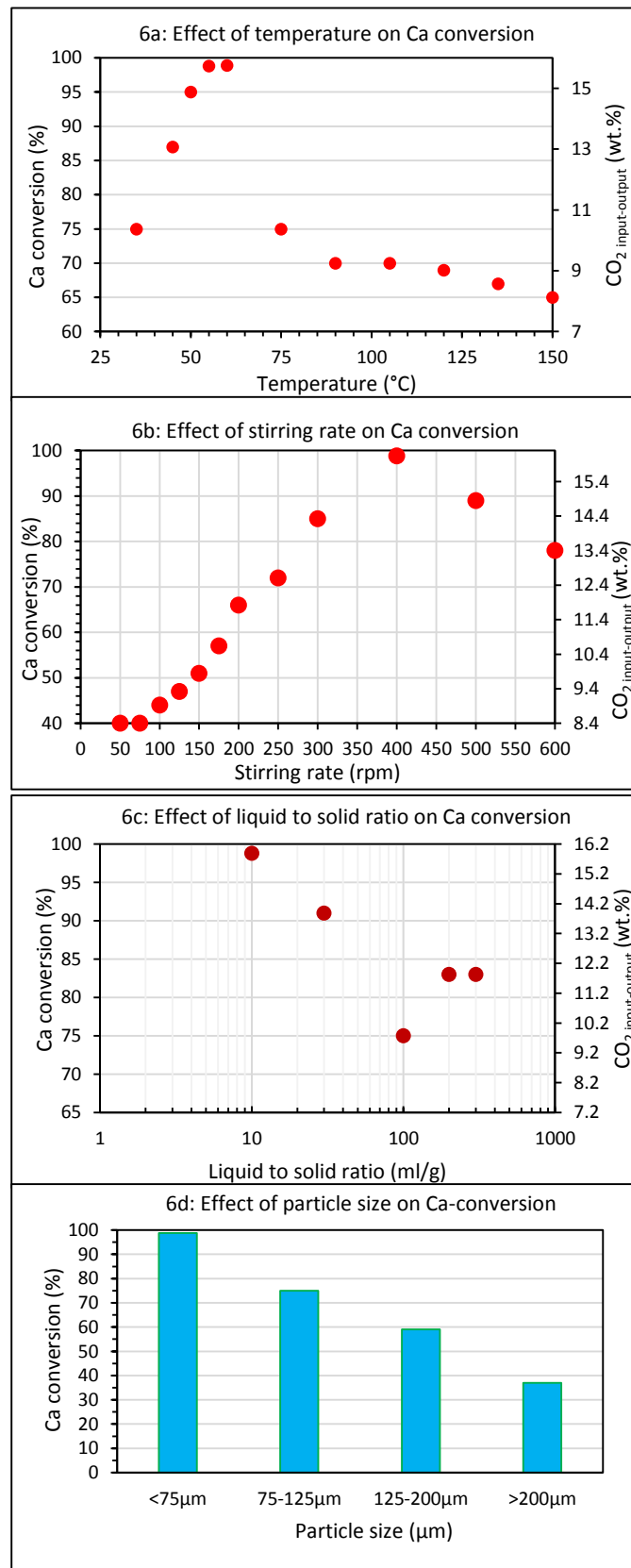


**Fig. 6** The effect of procedure variables (a) reaction temperature, (b) stirring rate, (c) liquid to solid ratio, and (d) particle size on conversion of Ca to  $\text{CaCO}_3$  in mineral carbonation process.

### Mass balance: the amount of Ca conversion

The XRF results revealed that the initial amount of calcium in the red gypsum samples averages at around 32.2% by mass. In each carbonation experiment, a fixed mass (10g) of gypsum was used for the quantitative reactions. The results showed that only calcium was involved in carbonation and the amount of  $\text{CaCO}_3$  produced during the carbonation step was 6.332g. The ICP-MS analysis revealed that the amount of  $\text{Ca}^{2+}$  precipitated as  $\text{CaCO}_3$  is 50.25%. The amount of Ca converted, which was determined from Equation 5, is therefore 98.8%.

TGA test was carried out on the final product obtained after the carbonation experiment on red gypsum sample and these results were supported by XRD analysis for the final product (See figure 5d). The reaction product was confirmed to be  $\text{CaCO}_3$  – mainly calcite with minor quantities of metastable vaterite. The peaks at  $26.84^\circ$  and  $39.72^\circ$  are assigned to vaterite, while peaks at  $23.50^\circ$ ,  $29.20^\circ$ ,  $31.32^\circ$ ,  $33.56^\circ$ ,  $40.88^\circ$ ,  $43.74^\circ$ ,  $48.08^\circ$ ,  $50.56^\circ$ , and  $56.88^\circ$  are assigned to calcite. Thermal analysis (TGA) confirms these findings and suggests the calcium carbonate produced is quite pure.

### Rate of $\text{CO}_2$ uptake

As described previously, the process variables such as reaction temperature, particle size, liquid to solid ratio, and stirring speed influence the rates of  $\text{CaCO}_3$  precipitation and  $\text{CO}_2$  uptake. Figure 6a shows the reaction temperature from  $25^\circ\text{C}$  to  $60^\circ\text{C}$  and its influence on  $\text{CO}_2$  uptake. The controlling mechanisms are dominated by the relative solubility of the compounds involved: gypsum (stable at low

temperatures) and anhydrite (stable at elevated temperatures) and the rather non-linear change of carbonate mineral and  $\text{CO}_2$  solubility with temperature.

Figure 7 illustrates that the rate of  $\text{CO}_2$  uptake for all particle sizes was highest within the first 15 minutes of reaction. The smallest particle size ( $d_{38} < 75 \mu\text{m}$ ) exhibits the highest rate of  $\text{CO}_2$  uptake as would be expected from its increased surface area

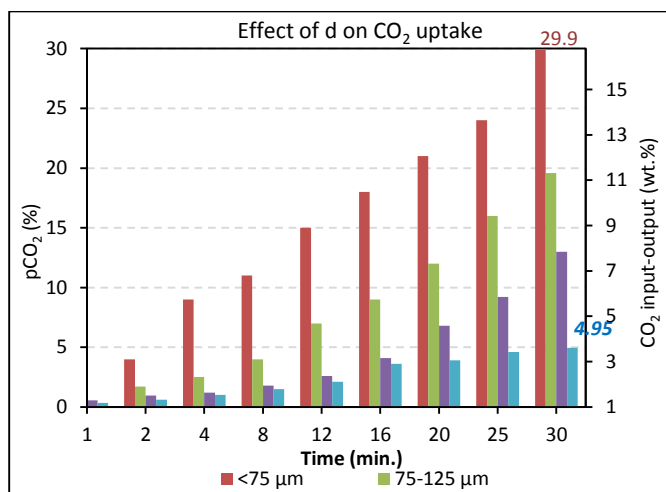


**Fig. 7** Plot of different particle sizes of carbonated red gypsum sample and volume of  $\text{CO}_2$  trapped during half an hour

**Table 2** The rate of  $\text{CO}_2$  uptake in the system based on the effect of variables

$\text{CO}_2$	Variables							
	T (K)				L/S (ml/g)			
	298.15 25 (°C)	323.15 50 (°C)	333.15 60 (°C)	348.15 75 (°C)	10	30	100	200
$\text{CO}_2$ in-out (%)	7	15	15.8	10.4	15.8	13.9	9.8	11.9
$\text{CO}_2$ uptake (mmol/g)	1.41	2.78	2.85	1.79	2.85	2.50	1.76	2.14
$\text{CO}_2$	Variables							
	n (rpm)				d (μm)			
	100	200	300	400	<75	75-125	125-200	>200
$\text{CO}_2$ in-out (%)	8.9	11.9	14.35	15.8	15.8	10.8	7	4.8
$\text{CO}_2$ uptake (mmol/g)	1.60	2.14	2.58	2.85	2.85	2.01	1.26	0.86

### Considerations for industrial scale-up

The calculations and data used in performing energy balance estimates for the process are shown in Supported Information D (SID1-SID3). We have previously shown that the amount of energy consumption for the mining procedure of by-product red gypsum is negligible. Moreover, the amount of energy consumption for operation of filtration and crushing is 0.25 and 0.643 (kWh/t  $\text{CO}_2$ ), respectively. Furthermore, the work index for red gypsum sample is considered to be 10.77 kWh/t, which involves the thermal decomposition of sample.

The amount and cost of chemicals needed for the mineral carbonation process of red gypsum are given in SID4. In the input route,  $\text{NH}_4\text{OH}$  is produced by dissolving equal amounts of  $\text{NH}_3$

solution and distilled water (e.g., 1 ml of water and 1 ml of  $\text{NH}_3$ ). Under conditions with the optimum L/S ratio of 10 ml/g, the cost of one tone of  $\text{CO}_2$  sequestration is 208.44 US\$ in this process. In these estimates, the highest costs are due to the  $\text{NH}_3$  solution and sulfuric acid requirements (i.e., 97.02 and 89.76 US\$), which are 46.5% and 43.1% of the total cost, respectively. It could be argued that the cost of raw materials is, in part, related to the rate of  $\text{CO}_2$  uptake. Additionally, the L/S ratio influences the amount of energy consumed. Because the rate of  $\text{CO}_2$  uptake decreases at the maximum L/S ratio more chemicals and raw materials are needed for storage of  $\text{CO}_2$ . Furthermore, the rates of dissolution and  $\text{CO}_2$  uptake influence the amount of products obtained and the chemicals needed, respectively. Consequently, analyzing the initial cost of mineral carbonation of red



gypsum suggests that the energy consumption and cost are minimized at the optimum L/S ratio.

Figure 8 shows a schematic for the carbonation process for sequestration of one t of carbon dioxide. As discussed before, approximately 1.251 t of by-product red gypsum, 2.72 t of  $\text{H}_2\text{SO}_4$ , and 4.62 t of  $\text{NH}_3$  solution are needed to sequester 1 t of  $\text{CO}_2$ . Consequently, 0.792 t of  $\text{CaCO}_3$  are produced as the main product during mineral carbonation process of by-product red gypsum. In addition, 0.086 and 0.350 t of the first and second products are collected, respectively. The sum of the all obtained products is 1.228 t, which is close to the preliminary amount of red gypsum used. Additionally, the reaction products have a marketable value in construction (See SID5), agriculture and other industries as they are essentially clean calcium carbonate.

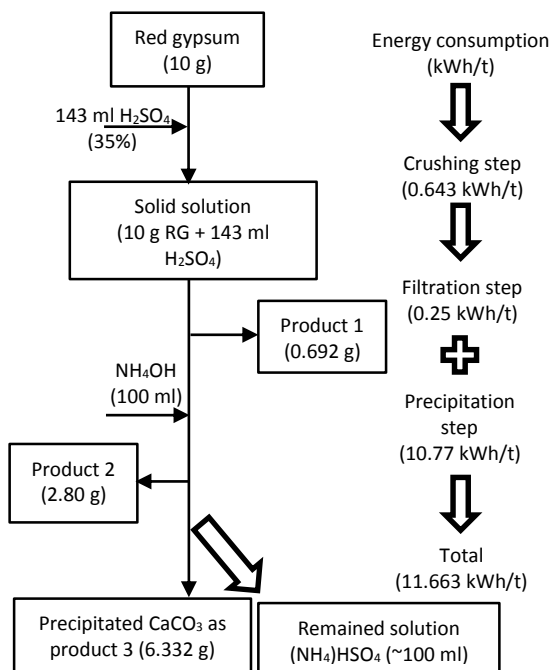


**Fig. 8** The scheme of carbonation process and energy consumption for sequestration of one tonne  $\text{CO}_2$

The amount of energy consumed in each step of the carbonation process is shown in Figure 8. On a larger scale, the precipitation step consumes 10.77 kWh/t energy in mineral carbonation, which is 92.34% of the total energy consumption. This step is considered to be the highest consumer of energy in the mineral carbonation process of red gypsum. After that, the steps of transportation and crushing use second and third highest amounts of energy.

The total cost of energy consumed for one t  $\text{CO}_2$  sequestration is given in SID6 and SID7. The highest cost is related to the precipitation step needed for this carbonation process is close to 92.66% of the total cost. Therefore, the total cost of 1 t of  $\text{CO}_2$  sequestration by mineral carbonation of by-product red gypsum is 62.35 US\$ (Fig. 9).

To make a complete estimate of the  $\text{CO}_2$  mass balance, should this process be adopted commercially, it is important to account for the embedded  $\text{CO}_2$  associated with the reactants consumed. A reasonable estimate of the  $\text{CO}_2$  embedded in  $\text{NH}_3$  would be 2 tonne  $\text{CO}_2$  generated per tonne of  $\text{NH}_3$  synthesized. This is mid-way in the range (1.6 to 3.2 t/t) quoted by the Intergovernmental Panel on Climate Change review of the ammonia and nitrate fertilizer industries published in 2006.

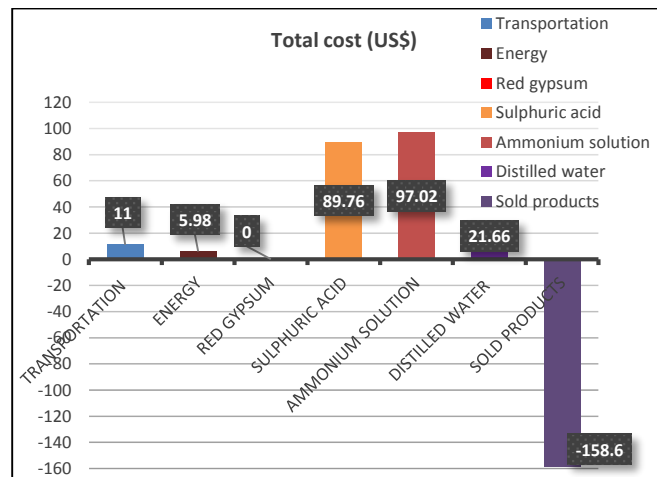


**Fig. 9** Chart diagram of total cost of 1 tonne  $\text{CO}_2$  sequestration for mineral carbonation of by-product red gypsum.

As discussed before, the amount of produced waste in the mineral carbonation process is considerable. Therefore, the waste that is produced needs to be reused in order to diminish environmental impacts. Moreover, reuse of products such as construction materials, could decrease the cost of  $\text{CO}_2$  sequestration by selling them. However, there is a limitation to the reuse of products due to their small grain size. Alternatively, cements need very fine particle sizes for additives. It could be suggested that the products could be reused as cement additives to reduce the environmental impact and the cost of the carbonation process.

The efficiency of  $\text{CO}_2$  sequestration of the mineral carbonation process is defined on the basis of the amount of  $\text{CO}_2$  sequestered in the carbonation reactor ( $\text{CO}_2$  sequestered) and the net overall amount of  $\text{CO}_2$  sequestered by the mineral carbonation process ( $\text{CO}_2$  avoided) [14]. The extra emission associated with the mineral carbonation process is determined by the power and heat consumption of the process. The total power and heat consumptions are 24 and 11 kWh/t  $\text{CO}_2$  sequestered, respectively. Based on electricity source, total  $\text{CO}_2$  emission of inputs in mineral carbonation of red gypsum is 15.08 kg  $\text{CO}_2$ /t  $\text{CO}_2$  sequestered. Therefore, the cost of  $\text{CO}_2$  avoided for mineral carbonation of red gypsum is 66.82 US\$/t  $\text{CO}_2$  avoided, respectively (see SID).

To verify the rate of sequestered, total dissolved inorganic carbon (TDIC) was determined as carbon in a gas sample taken from gas-tight cylinder and in a sample after mineral carbonation process. The amount of TDIC (i.e.,  $3.9 \times 10^{-5}$  mmol) was calculated by applying Henry's law considering the known volumes of headspace and solution (see SID). The amount of TDIC is too small and the effect of this amount on the rate of  $\text{CO}_2$  uptake is not considered.

### Environmental issues

There are three main environmental issues associated with the mineral carbonation process of by-product red gypsum:

- (1) Production of a lot of waste during carbonation process.
- (2) Presence of impurities in the feedstock and  $\text{CO}_2$ .
- (3) Effect of cost in choosing feasible technique for the carbonation process.

As discussed before, 0.086 t of the first waste product is produced by sequestering 1 t of  $\text{CO}_2$  via the mineral carbonation of red gypsum. This amount also involves some impurities, which are not dissolved in sulfuric acid dissolution step. In addition, selecting the mineral carbonation technique should be feasible based on cost

because the carbonation process with the lowest cost could possibly increase the environmental impact. As a result, the first product, which is rich in TiO<sub>2</sub>, can be reused as a construction matter in the roads, chemical manufacturing plants, nuclear power plants, and heating-cooling systems. Additionally, the second product could be applied in the iron factory due to high amount of Fe. Furthermore, the third product (CaCO<sub>3</sub>) and rest solution [(NH<sub>4</sub>)HSO<sub>4</sub>] are used in the agriculture and TiO<sub>2</sub> factories, respectively. Therefore, the effect of two first environmental issues could be resolved as discussed.

There is a remarkable possibility of reusing the products of mineral carbonation of red gypsum in construction, which positively influences the environmental impact. For example, the characterizations of construction could be improved by the use of products obtained via carbonation process. The use of feedstocks such as red gypsum in concrete and asphalt is hindered by hydration of CaO (and as well MgO in other feedstocks). Therefore, the mineral carbonation of red gypsum causes the conversion of CaO to CaCO<sub>3</sub> and prevents this problem, which is considered an advantage for environmental impacts.

In addition to its GHG effects, CO<sub>2</sub> sequestration presents another environmental issue. In the case of natural minerals, large-scale excavation of mines has a considerable environmental impact. However, for industrial by-products such as red gypsum, this effect is negligible because no mining is needed.

Low cost and energy required in the use of by-product red gypsum were considered to be impressive advantages for CO<sub>2</sub> sequestration process. Therefore, acceptable cost and energy required confirmed that using this feedstock is also applicable and feasible for mineral carbonation process.

## Conclusions

By performing the dissolution and carbonation experiments of red gypsum samples in two stages, the applicability and feasibility of this process were initially investigated for CO<sub>2</sub> mineral carbonation:

- (1) At the end of the carbonation experiment, CaCO<sub>3</sub> was produced from the reaction of CO<sub>2</sub> and Ca-rich solution. It was determined that precipitation of CaCO<sub>3</sub> using red gypsum is completely feasible and applicable for mineral carbonation process.
- (2) Wide-range conditions of procedure variables such as temperature, particle size, stirring rate, and liquid to solid ratio were investigated in these experiments. By considering the optimum amount of these variables, the maximum amount of Ca conversion was determined.
- (3) The low cost and small amount of energy required in the use of red gypsum were considered to be impressive advantages of the CO<sub>2</sub> sequestration process. Therefore, the acceptable costs and energy required for the mineral carbonation process of red gypsum confirmed that using red gypsum is also applicable and feasible for mineral carbonation process without any considerable environmental impact.
- (4) The main environmental issue was related to production of impurities in the first and second waste products for sequestration of 1 t of CO<sub>2</sub> using the mineral carbonation process of red gypsum. This environmental impact could be reduced by reuse of these products in industries and factories.

## Acknowledgements

This work was funded and supported by the Ministry of Education Malaysia (MOE) with the Vote No. Q.J130000.2542.06H2 and Universiti Teknologi Malaysia (UTM). The authors are also grateful to Sahar Zarza for appreciating her work and positive comments.

## Notes and references

<sup>a</sup> Department of Petroleum Engineering, Faculty of Petroleum and Renewable Energy Engineering, Universiti Teknologi Malaysia, 81310 UTM, Johor, Malaysia.

Email: [romeid2@live.utm.my](mailto:romeid2@live.utm.my); [omeidrahmani@gmail.com](mailto:omeidrahmani@gmail.com)

H/P.: +60147217584

<sup>b</sup> Islamic Azad University, Mahabad Branch, Mahabad, Iran.

<sup>c</sup> Mineral Industry Research Organisation, Wellington House, Starley Way, Birmingham International Park, Solihull, Birmingham, B37 7HB, United Kingdom.

<sup>†</sup>Electronic Supplementary Information (ESI) available: See DOI: 10.1039/b000000x/

- 1 S. Tian, J. Jiang, K. Li, F. Yan and X. Chen, *RSC Adv.*, 2014, **4**, 6858.
- 2 J. Gibbins and H. Chalmers, *Energy Policy*, 2008, **36**, 4317.
- 3 K. Z. House, D. P. Schrag, C. F. Harvey and K. S. Lackner, *Proceedings of the National Academy of Sciences*, 2006, **103**, 12291.
- 4 H. E. King, O. Plümper and A. Putnis, *Environ Sci. Technol.*, 2010, **44**, 6503.
- 5 J. Highfield, H. Q. Lim, J. Fagerlund and R. Zevenhoven, *RSC Adv.*, 2012, **2**, 6535.
- 6 D. H. Chu, M. Vinoba, M. Bhagiyalakshmi, I. H. Baek, S. C. Nam, Y. Yoon, S. H. Kim and S. K. Jeong, *RSC Adv.*, 2013, **3**, 21722.
- 7 S. Zendejboudi, A. Bahadori, A. Lohi, A. Elkamel and I. Chatzis, *Energy & Fuels*, 2013, **27**, 401.
- 8 K. S. Lackner, C. H. Wendt, D. P. Butt, E. L. Joyce and D. H. Sharp, *Energy*, 1995, **20**, 1153.
- 9 S. Zendejboudi, A. Khan, S. Carlisle and Y. Leonenko, *Energy & Fuels* 2011, **25**, 3323.
- 10 A. Azdarpour, M. Asadullah, R. Junin, M. Manan, H. Hamidi and E. Mohammadian, *Fuel Process. Tech.*, 2014, **126**, 429.
- 11 O. Rahmani, R. Junin, M. Tyrer and R. Mohsin, *Energy & Fuels*, 2014, Article ASAP, DOI: 10.1021/ef501265z
- 12 M. G. Lee, Y. N. Jang, K. W. Ryu, W. Kim and J. H. Bang, *Energy*, 2012, **47**, 370.
- 13 A. A. Olajire, *J Petrol Sci. Eng.*, 2013, **109**, 364.
- 14 W. J. J. Huijgen, G. J. Witkamp and R. N. J. Comans, *Environ Sci. Technol.*, 2005, **39**, 9676.
- 15 P. Claisse, E. Ganjian and M. Tyrer, *The Open Construction and Building Technology Journal*, 2008, **2**, 294.
- 16 S. J. T. Hangx and C. J. Spiers, *Int. J Greenhouse Gas Control*, 2009, **3**, 757.
- 17 S. Fauziah, T. Zauyah and T. Jamal, *Sci. Total Environ*, 1996, **188**, 243.
- 18 M. J. Gazquez, J. P. Bolivar, F. Vaca, R. García-Tenorio and A. Caparros, *Cement & Concrete Composites*, 2013, **37**, 76.
- 19 A. A. Park and L. Fan, *Chem. Eng. Science*, 2004, **59**, 5241.
- 20 H. M. J. Bearat, M. J. McKelvy, A. V. G. Chizmeshya, D. Gormley, R. Nunez, R. W. Carpenter and et al., *Environ Sci. Technol.*, 2006, **40**, 4802.